Polymer Degradation and Stability 240 (2025) 111495

Contents lists available at ScienceDirect

Polymer Degradation and Stability

journal homepage: www.journals.elsevier.com/polymer-degradation-and-stability

Synergistic flame retardant coatings for carbon fibre-reinforced ε-caprolactam-based polyamide 6 composites: Fire performance and mechanical properties

Zsófia Kovács [a,b], Andrea Toldy [a,b,*]

[a] Department of Polymer Engineering, Faculty of Mechanical Engineering, Budapest University of Technology and Economics, H-1111, Budapest, Műegyetem rkp. 3, Hungary
[b] MTA-BME Lendület Sustainable Polymers Research Group, H-1111, Budapest, Műegyetem rkp. 3, Hungary

ARTICLE INFO

Keywords:
Polyamide 6 composites
Anionic ring-opening polymerisation
Carbon fibre reinforced composites
Flame retardancy
In-mould coating

ABSTRACT

The use of long fibre-reinforced thermoplastic composites is increasing, but a significant drawback is their flammability due to the organic matrix. This study explores the flame retardancy of carbon fibre-reinforced PA6 composites coated via in-mould coating. The matrix and coating were made by anionic ring-opening polymerisation of ε-caprolactam. The flame retardants used were magnesium oxide (MgO), red phosphorus (RP), hexaphenoxycyclotriphosphazene (HPCTP) and expandable graphite (EG). The flammability and fire performance were evaluated using pyrolysis-combustion flow calorimetry (PCFC), mass loss type cone calorimetry, and glow wire flammability index (GWFI) testing, while evolved gases were analysed using laser pyrolysis coupled with Fourier transform infrared spectrometry (LP-FTIR). Scanning electron microscopy (SEM) and energy dispersive X-ray spectroscopy (EDS) analysis of the solid residues post-combustion revealed the mechanisms responsible for flame retardancy. Flame retardant coatings reduced the peak heat release rate by up to 33 % and the total heat release by up to 40 % compared to the reference sample. The combination of flame retardants containing magnesium or phosphorus with expandable graphite resulted in a synergistic flame retardant effect due to the enrichment of the heteroatoms in the outer char layers, contributing to a more stable intumescent char and protective barrier layer. The LP-FTIR analysis indicated reduced emissions of toxic gases, particularly hydrogen cyanide (HCN) and carbon monoxide (CO), furthermore, it was found that flame retardants reduced the intensity of the peaks associated with C-H vibrations and P-related peaks appeared in the presence of HPCTP and RP. Overall, the combined flame retardant coatings improved the fire safety of carbon fibre-reinforced PA6 composites without compromising mechanical properties and mitigated the negative effect of carbon fibres on char formation.

1. Introduction

The use of continuous fibre-reinforced thermoplastic matrix composites is significant in many industrial sectors, including the transport industry. By replacing conventional metal parts, continuous fibre-reinforced thermoplastic composites allow significant weight reduction and increased fuel efficiency, which is important from an economic and environmental point of view [1–4]. They also offer the advantage of easier recyclability compared to thermoset matrix composites, as the matrix can be remelted after grinding to produce a new product [5–7].

Polyamide 6 (PA6) is particularly noteworthy among thermoplastic matrices because of its high strength and excellent chemical resistance [8,9]. Continuous fibre-reinforced PA6 composites can be produced by anionic ring-opening polymerisation (AROP), where the low viscosity (3–5 mPa·s) caprolactam (CL) monomer is mixed with an activator and an initiator and polymerisation takes place within a few minutes (~5 min) [10,11]. With this technology, continuous fibre-reinforced composites can be easily produced since the polymerisation takes place in the mould between the reinforcing materials. A major advantage of the reaction is that it occurs at a lower temperature (140-160 °C) than the melting point of PA6 (220 °C) [12].

Due to safety regulations, the flame retardancy of PA6-based composites is an essential requirement, especially in applications such as transport, electrical and electronics, and construction [13]. PA6 exhibits

* Corresponding author.
E-mail address: atoldy@edu.bme.hu (A. Toldy).

https://doi.org/10.1016/j.polymdegradstab.2025.111495
Received 16 April 2025; Received in revised form 13 June 2025; Accepted 13 June 2025
Available online 15 June 2025

dripping and rapid flame spread during combustion, which limits its application in cases where it meets stringent fire safety requirements. The flame retardancy of composites created by anionic ring-opening polymerisation is an area of increasing research [14]. However, anionic polymerisation is sensitive to many compounds, including flame retardants [15]. According to the literature [16,17], the phosphorus-containing, bulkier heterocyclic hexaphenoxycyclotriphosphazene is a promising flame retardant, capable of significantly reducing the maximum heat release and achieving a V-0 rating according to UL-94. Furthermore, the combination of flame retardants offers an effective solution, as the synergistic effect can notably enhance the flammability properties. One approach to incorporating flame retardants is applying them directly to the matrix. However, several issues can arise as solid particle flame retardants can be filtered out by the reinforcing material. Furthermore, delamination may occur due to the action of flame retardants in the condensed phase. It is also a key challenge that in the case of intumescent flame retardants acting in the condensed phase, the flame retardant action is largely hindered by the reinforcement layers [18,19]. Using flame retardant coatings is a way to overcome these problems [20]. Various methods for applying coatings exist, such as brushing, spraying or in-mould coating. Of these, in-mould coating may be the most advantageous, as polymerisation and, thus the formation of the coating takes place in the closed mould [21].

This publication is based on our previous articles [22,23]. However, the innovation of this publication lies in the fact that we complement the flammability of previously prepared coated composites and comprehensively investigate the mechanism while also analysing the mechanical properties of the composites. In this study, carbon fibre-reinforced PA6 composites were prepared through anionic ring-opening polymerisation. The surface of the composites was coated using in-mould coating to form a flame retardant layer. The flammability of the coatings was evaluated by pyrolysis-combustion flow calorimetry (PCFC), and evolved gases were analysed by laser pyrolysis coupled with Fourier transform infrared spectrometry (LP-FTIR). The fire performance of the coated composites was assessed using mass loss type cone calorimetry (MLC) and glow wire flammability index (GWFI) testing. The solid residue after combustion was analysed by SEM-EDS, and combined with the detected gas phase decomposition products from pyrolysis, this data was used to evaluate the flame retardancy mechanism. Additionally, the adhesion between the surface and coating, as well as the mechanical properties of the coated composites, were investigated.

2. Materials and methods

2.1. Materials

For the preparation of the matrix and the coating, *AP-NYLON Caprolactam* type ε-caprolactam (CL, L. Brüggemann GmbH & Co. KG, Heilbronn, Germany) was used as a monomer. Hexamethylene-1,6-dicarbamoyl caprolactam, brand name *Bruggolen C20P* (C20, L. Brüggemann GmbH & Co. KG, Heilbronn, Germany), was used as an activator, while sodium dicaprolactamato-bis-(2-methoxyethoxo)-aluminate type activator, brand name *Dilactamate* (DL, Katchem, Prague, Czech Republic), was used as an initiator. *PX 35 UD 300* type unidirectional carbon fibre reinforcement (CF, Zoltek Zrt., Nyergesújfalu, Hungary) was used as the reinforcing material for the composites. The flame retardants used were magnesium oxide (MgO, Sigma Aldrich, Budapest, Hungary), *Exolit RP607* type red phosphorus (RP, Clariant, Muttenz, Switzerland), Rabitle FP110 hexaphenoxycyclotriphosphazene (HPCTP, Fushimi Pharmaceutical Co Ltd., Japan) and *ES 100 C10* type expandable graphite (EG, Graphit Kropfmühl, Hauzenberg, Germany). RP is a red powder with a phosphorus content higher than 95 %. In the case of EG, it expands with heat and forms "worm-like" formations. The volume change during expansion is 100 cm^3/g, while the initial degradation temperature is 200 °C. The HPCTP is a white powder with a phosphorus content of 13.4 %. The selected flame retardant compositions were determined based on our previous research [22,23] and are listed in Table 1. For the HPCTP-containing samples, the amount of HPCTP was not expressed as mass%, but was characterised by the P-content commonly used in the literature. 3 P % HPCTP corresponds to 22.38 g HPCTP/100 g polymer.

Table 1
The flame retardant compositions used.

Sample name	MgO [%]	RP [%]	HPCTP [P %]	EG [%]
PA6	-	-	-	-
PA6/5 %MgO/5 %EG	5	-	-	5
PA6/5 %RP/5 %EG	-	5	-	5
PA6/3P %HPCTP/3 %EG	-	-	3	3
PA6/3P %HPCTP/4 %EG	-	-	3	4

2.2. Preparation of flame retardant PA6

Reference and the flame retardant PA6 coatings (without composite) were fabricated according to the procedure shown in Fig. 1. First, the aluminium mould with 100 mm x 100 mm x 2 mm cavity was cleaned with methanol, closed and preheated to 150 °C in a *UT6*-type drying oven (Heraeus Holding GmbH, Hanau, Germany). While the mould was heating, CL and C20, along with the flame retardants for flame retardant samples, were measured, and then melted and mixed using an *MR Hei-TEC* type (Heidolph Scientific Products GmbH, Schwabach, Germany) magnetic stirrer. After the addition of DL, the mixed CL system was injected into the closed mould using a *1025 TLL 25ml SYR* type heat-resistant Hamilton syringe (Hamilton Company, Reno, Nevada) and the mould was removed from the drying oven after 15 min. The mould was left to cool at room temperature.

2.3. Preparation of PA6/CF composites

A small-scale implementation of the T-RTM manufacturing technology was used to produce the composites (Fig. 2). We used an aluminium mould with a 100 mm x 100 mm x 2 mm mould cavity, in which 5 layers of unidirectional CF reinforcement were pre-placed in $[0]_5$ layups. After closing, the mould was placed in a *UT6*-type drying oven (Heraeus Holding GmbH, Hanau, Germany) at 150 °C. The CL was mixed with C20 and melted using an *MR Hei-TEC* type (Heidolph Scientific Products GmbH, Schwabach, Germany) magnetic stirrer, and after adding the DL, the CL solution, which resembled the viscosity of water, was then injected into the closed mould using a *1025 TLL 25ml SYR* type heat-resistant Hamilton syringe (Hamilton Company, Reno, Nevada). The anionic ring-opening polymerisation occurred in the closed mould between the reinforcing materials. The mould was removed from the oven after 15 min and left to cool at room temperature.

2.4. Preparation of flame retardant coating for PA6/CF composites

The coating was prepared by in-mould coating (Fig. 3). The composite prepared as described in section 2.2 was placed in an aluminium mould with a 100 mm x 100 mm x 2.5 mm mould cavity, and after closing the mould, it was preheated at 150 °C in a *UT6* type drying oven (Heraeus Holding GmbH, Hanau, Germany). The CL and C20 were mixed with the flame retardants and melted at 120 °C using a magnetic stirrer *MR Hei-TEC* (Heidolph Scientific Products GmbH, Schwabach, Germany). DL was added once the mixture was melted entirely and injected into the closed mould using a *1025 TLL 25ml SYR*-type heat-resistant Hamilton syringe (Hamilton Company, Reno, Nevada). The anionic ring-opening polymerisation was carried out in the mould, and a 0.5 mm thick CL-based flame retardant coating was formed on the upper part of the composite surface. The mould was removed from the drying

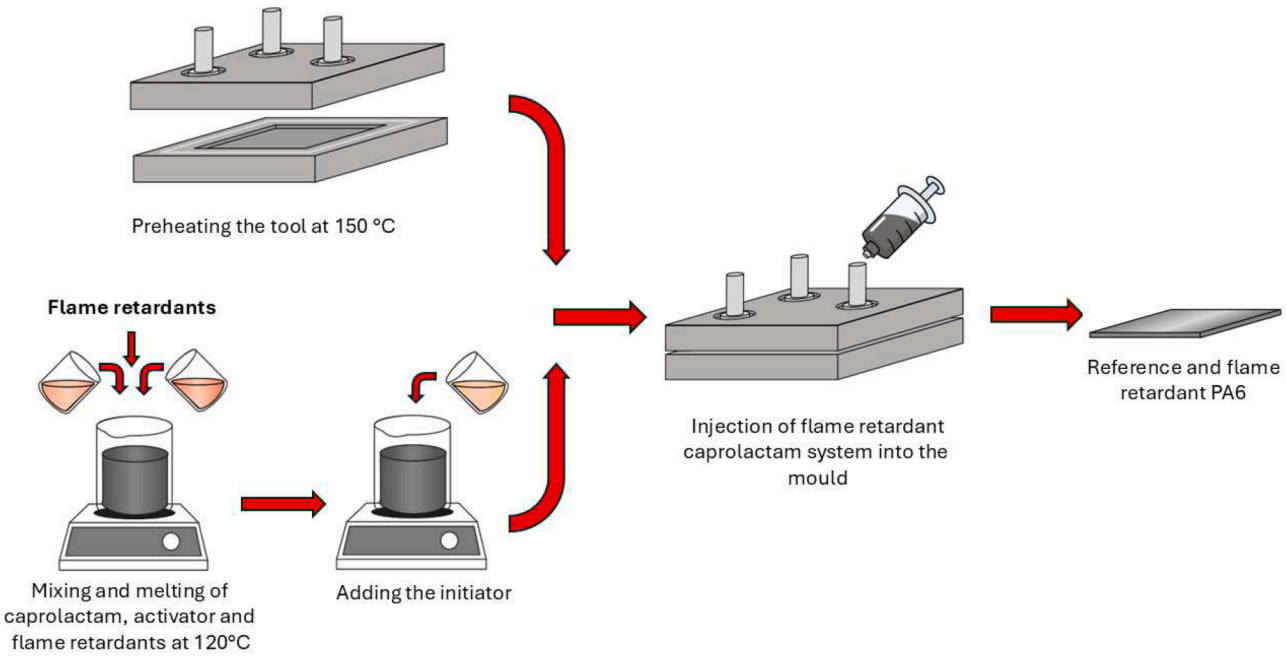

Fig. 1. Preparation stages of reference and flame retardant polyamide 6.

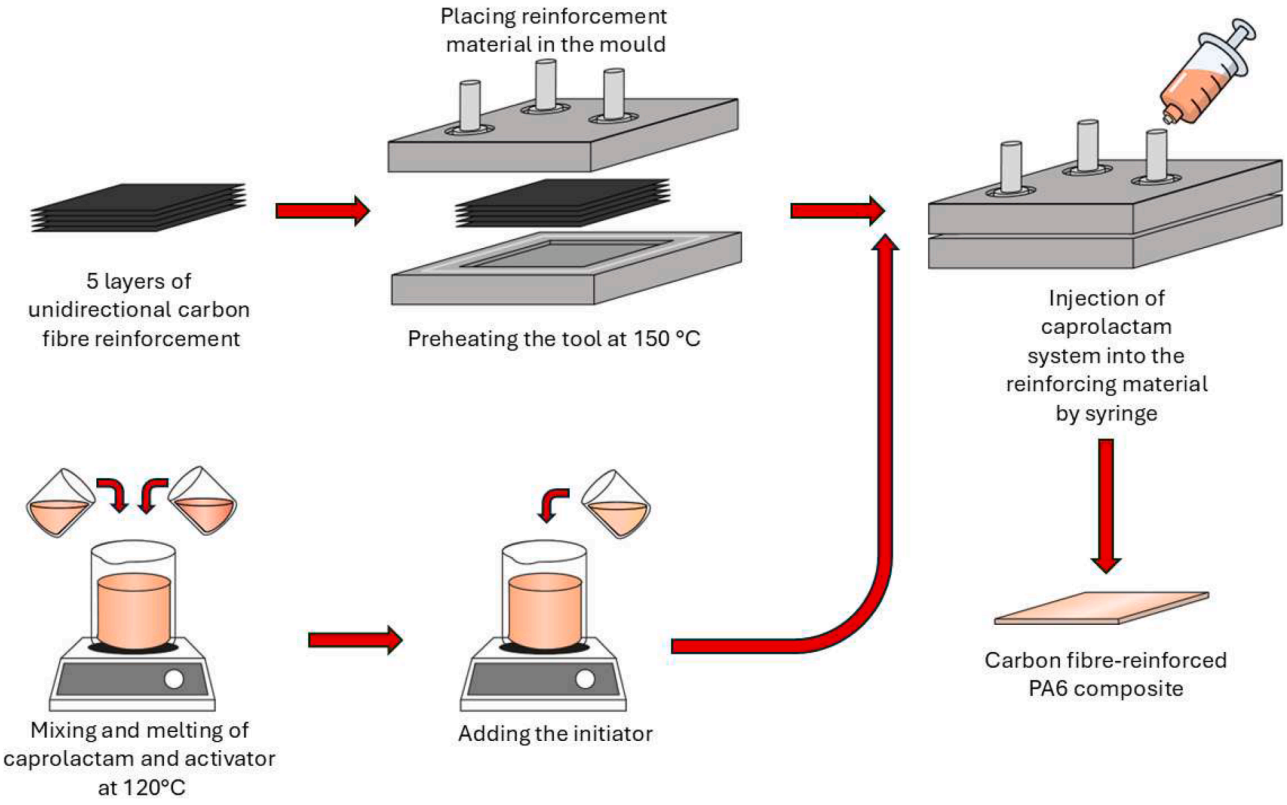

Fig. 2. Preparation stages of carbon fibre reinforced polyamide 6 composites.

oven after 15 min and left to cool at room temperature.

2.5. Characterisations

2.5.1. Pyrolysis-combustion flow calorimetry (PCFC)

The flammability of the coatings alone (without composite) was tested with pyrolysis-combustion flow calorimetry (PCFC, Fire Testing Technology, East Grinstead, UK). Measurements were performed according to ASTM D-7309 at a heating rate of 1 °C/s on 8-10 mg samples. The maximum pyrolysis temperature was 750 °C, and the firing temperature was 900 °C. During the test, nitrogen and oxygen flow rates were 80 ml/min and 20 ml/min, respectively.

2.5.2. Mass loss type cone calorimetry (MLC)

The flammability of the coated composite samples was tested by mass loss type cone calorimetry (MLC, Fire Testing Technology, East

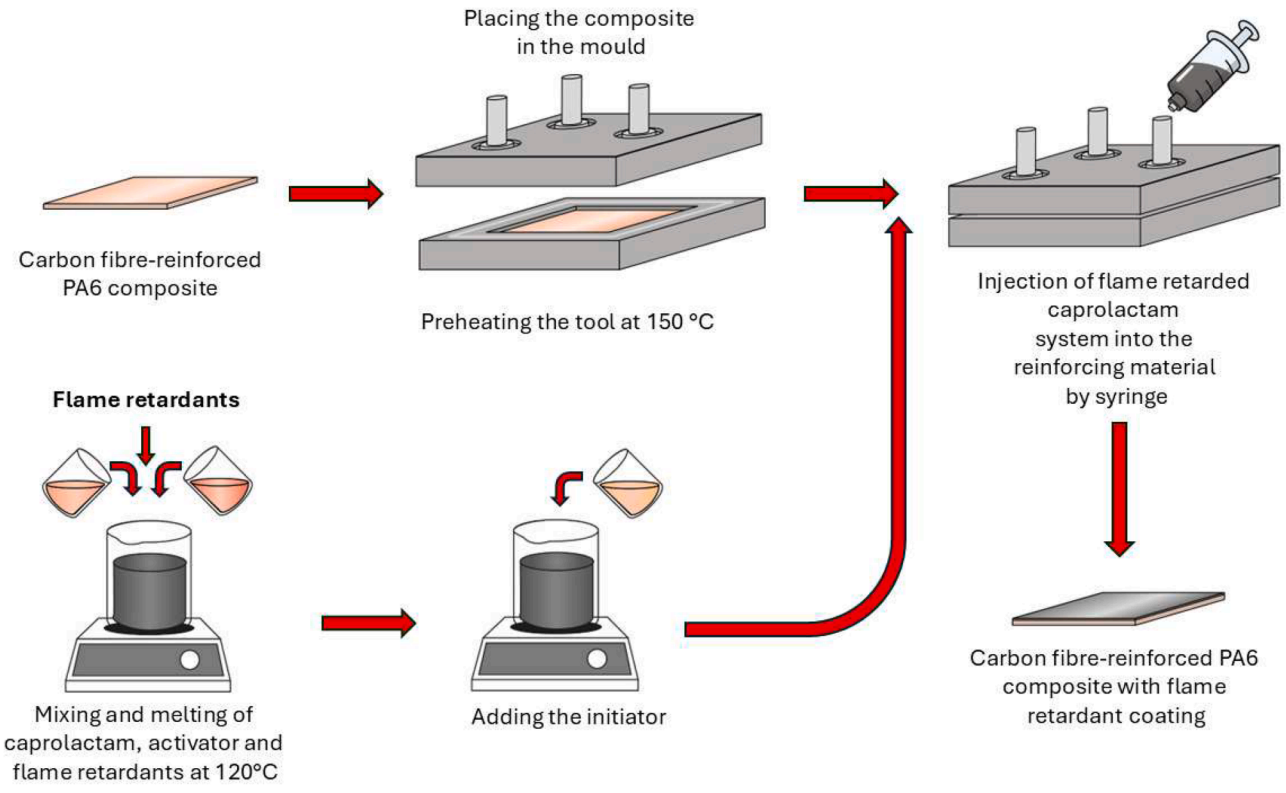

Fig. 3. Preparation stages of flame retardant coating for carbon fibre reinforced polyamide 6 composites.

Table 2
PCFC results for reference and flame retardant coatings.

Sample	pHRR [W/g]	t_{pHRR} [s]	THR [kJ/g]	HRC [J/g·K]	Residue [%]
PA6	416 (1st peak)	343	28	433	1.7
PA6/5 %MgO/5 %EG	309 (2nd peak)	440	22	436	16.1
PA6/5 %RP/5 %EG	355 (2nd peak)	510	22	381	9.7
PA6/3P %HPCTP/3 %EG	249 (1st peak)	368	26	443	2.6
PA6/3P %HPCTP/4 %EG	276 (2nd peak)	455	25	412	5.1

pHRR: peak heat release rate, t_{pHRR}: time to peak heat release rate, THR: total heat release, HRC: heat release capacity; Average standard deviation of the measured mass loss calorimeter values: pHRR: ±20; t_{pHRR}: ±5; THR: ±3; HRC: ±10; residue: ±2

Grinstead, UK) based on the ISO 13927 standard. The test was carried out on 100 mm x 100 mm specimens, where the reference (uncoated) composite had a thickness of 2 mm and the coated specimens had a thickness of 2.5 mm. A spark igniter was used to ignite the samples, and the heat flux was 50 kW/m^2. The time to ignition (TTI), the peak heat release rate (pHRR), the time to pHRR (t_{pHRR}), the total heat release (THR) and the residual mass were determined. In addition, the maximum average rate of heat emission (MARHE) and the effective heat of combustion (EHC) were calculated.

2.5.3. Scanning electron microscopy and energy dispersive X-ray spectroscopy (SEM-EDS)

After MLC testing, the residues of the reference and flame retardant-coated composites were examined using a JEOL JSM 6380LA scanning electron microscope (SEM, Jeol Ltd., Tokyo, Japan). The samples were gold-coated to avoid charging using a Jeol JPC1200 cathodic sputtering gold plating apparatus (Jeol Ltd., Tokyo, Japan). The residues were mapped using scanning electron microscopy with energy dispersive spectrometry (SEM-EDS) at 500x magnification. In the elemental analysis, both the inner and outer layers of the residue were analysed.

2.5.4. Laser pyrolysis - Fourier transform infrared spectrometry (LP-FTIR)

LP-FTIR was used to detect the gases generated during the pyrolysis of the coatings. The samples were pyrolysed using a SYNRAD 48-1 adjustable power CO_2 laser (Novanta Inc., Bedford, USA) and the spectra of the gases generated were recorded using a Bruker Tensor 37 FTIR (Bruker, Billerica, USA). The samples were pyrolysed for 1 min at 1 W power. The size of the samples was 20 mm x 10 mm x 2 mm.

2.5.5. Glow wire flammability index (GWFI)

The extinguishing capability of the coated composites was tested with a Glow Wire Tester T4-08 (Testing d. o. o., Slovenia). The measurement was carried out according to the IEC 60695 standard on test specimens with an area of 60 mm x 60 mm. The reference sample was 2 mm thick, while the coated samples were 2.5 mm thick. GWFI expresses the highest temperature at which the material is extinguished in 30 s after 30 s of contact with the glow wire.

2.5.6. Shore D hardness

The Shore D hardness of the reference PA6 and flame retardant coatings was determined using a Zwick H04.3150.000 hardness tester (Zwick GmbH & Co. KG, Ulm, Germany) according to ISO 48-2:2018. The test was carried out on 6 mm thick samples with a load of 50 N. 10 measuring points were taken on the samples.

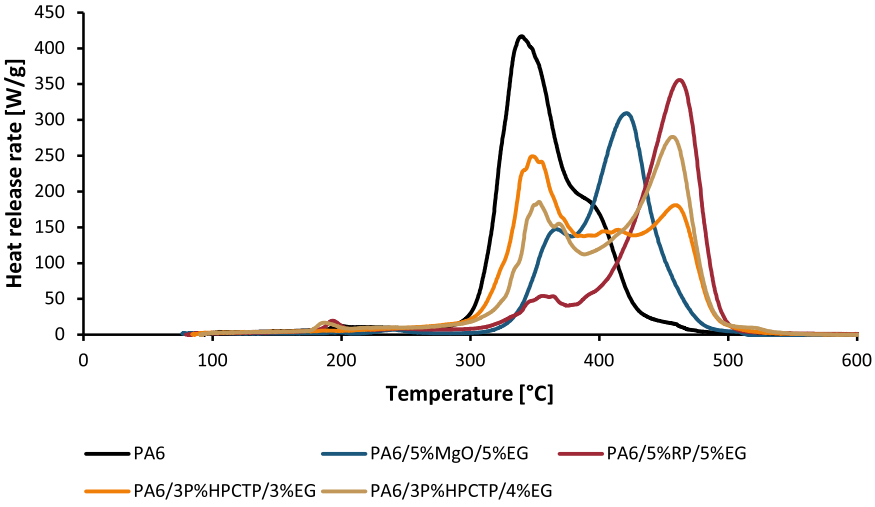

Fig. 4. Heat release curves as a function of temperature for pyrolysis-combustion flow calorimetry.

Table 3
MLC results of reference and PA6 composite with flame retardant coating.

Sample	TTI [s]	pHRR [kW/m^2]	t_{pHRR} [s]	THR [MJ/m^2]	Residue [%]	MARHE [kW/m^{2}s]	EHC [MJ/kg]
PA6/CF	17	347	164	95	32.5	255	67
PA6/CF/5 %MgO/5 %EG	21	252	65	68	40.7	181	45
PA6/CF/5 %RP/5 %EG	24	274	62	60	44.2	190	36
PA6/CF/3P %HPCTP/3 %EG	22	231	165	60	41.6	164	33
PA6/CF/3P %HPCTP/4 %EG	36	261	92	57	41.5	166	32

TTI: time to ignition, pHRR: peak heat release rate, t_{pHRR}: time to peak heat release rate, THR: total heat release, MARHE: maximum average rate of heat emission, EHC: effective heat of combustion; Average standard deviation of the measured mass loss calorimeter values: TTI: ±3; pHRR: ±30; t_{pHRR}: ±5; THR: ±3 residue: ±2

2.5.7. *Pull-off test*

The adhesion between the composite and the flame retardant coating was evaluated by pull-off test carried out according to ISO 4624/2016 using a DeFelsko PosiTest AT-M (DeFelsko Corporation, New York, USA). The diameter of the dollies used for the test was 20 mm. Before glueing the dollies, both the coating and the surface of the dollies were cleaned with methanol. The dollies were then fixed to the coating with Araldite 2011 two-component adhesive and left to cure for 24 h. In the next step, the dollies were cut around with the cutting tool provided with the equipment, and the test was performed using the test device. During the test, the device gives the pull-off strength value in MPa between the composite and the coating based on the diameter of the glued dolly. A preload of 0.7 MPa was applied during the test.

2.5.8. *Three-point bending test*

The three-point bending of the flame retardant coated composites

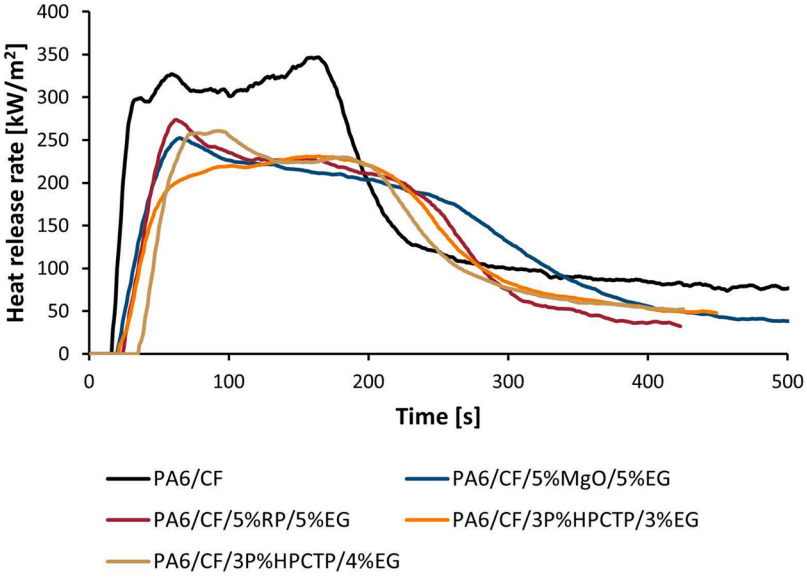

Fig. 5. Heat release rate of reference and flame retardant coatings in MLC measurements.

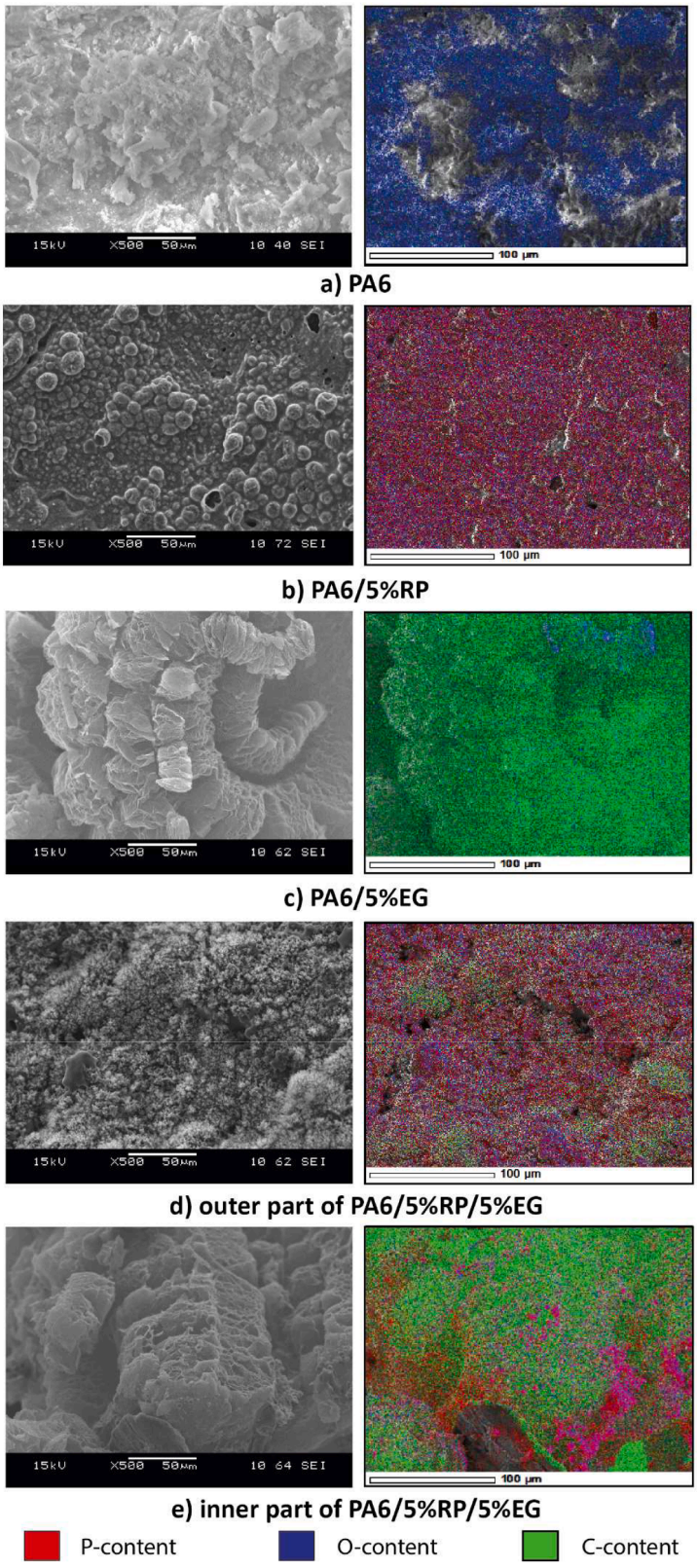

Fig. 6. SEM-EDS image of post-combustion residue where a) PA6, b) PA6/5 %RP, c) PA6/5 %EG, d) outer part of PA6/5 %RP/5 %EG, e) inner part of PA6/5 %RP/5 %EG.

was carried out on a Zwick Z005 type (Zwick GmbH & Co. KG, Ulm, Germany) bending machine according to DIN EN ISO 14125. The 80 mm x 10 mm x 2 mm reference composite and the 80 mm x 10 mm x 2.5 mm coated specimens were bent at 2 mm/min speed with a support distance of 64 mm, with the coating always on the pressed side. The measurement was taken up to the limit deflection, 10 % of the support, i.e. 6.4 mm. The limit bending stress and the flexural modulus were calculated using the Eqs. (1) and (2).

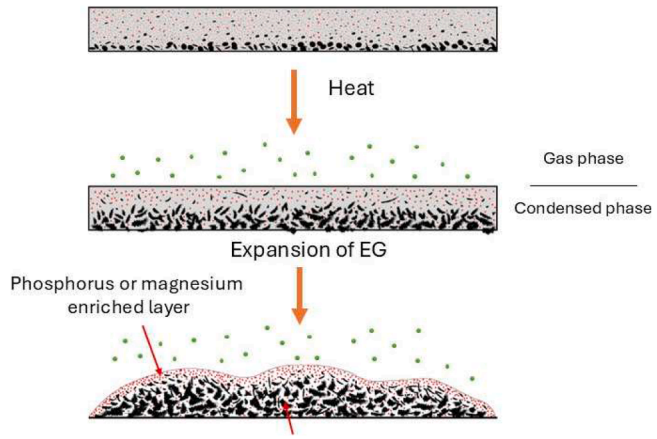

Fig. 7. Schematic diagram of the expansion of expandable graphite in the coating.

$$\sigma_h = \frac{3 \cdot F \cdot L}{2 \cdot b \cdot h^2} \quad (1)$$

where σ_h is the limit bending stress [MPa], F is the measured force value [N], L is the support distance [mm], b is the specimen width [mm], h is the specimen thickness [mm].

$$E_h = \frac{\sigma_2 - \sigma_1}{\varepsilon_2 - \varepsilon_1} \quad (2)$$

where E_h is the flexural modulus of elasticity [MPa], σ_1 is the stress value for 0.05 % relative deformation (ε_1) [MPa], σ_2 is the stress value for 0.25 % relative deformation (ε_2) [MPa].

3. Results and discussion

In our research, selected flame retardant formulations based on our previous publications [22,23] were applied as coatings on carbon fibre reinforced PA6 composites. In the first phase of the study, the flammability and hardness of the selected flame retardant compositions were investigated, followed by the flammability, mechanical properties and adhesion of the coated composites.

3.1. Pyrolysis-combustion flow calorimetry

The flammability of flame retardant PA6 coatings (without the composite) was tested with PCFC (Table 2 and Fig. 4). The samples were cut out in the cross-section of the specimen in such a way that the cut-out represents a uniform distribution of the additives. Cross-sectional directional sampling ensures that the distribution of additives corresponds to the average composition of the whole sample. The heat release rate curves (Fig. 4) show that PA6 exhibits a curve with a high peak value, which starts to develop around 300 °C. Under the influence of flame retardants, this peak decreases significantly and shifts slightly towards higher temperatures. In addition, a distinct second peak is formed, which has a higher heat release than the first peak (except for PA6/3P %HPCTP/3 %EG). For samples containing HPCTP and EG, the intensity of the first peak decreases with increasing EG content. With lower EG content, the expansion is less, so the decomposition proceeds faster. As shown in Table 2, compared to the peak heat release rate (pHRR) value for reference PA6 (416 W/g), each flame retardant decreased the pHRR. 3P % HPCTP and 3 % EG can reduce the pHRR by up to 40 %. In addition, the total heat release (THR) value was also reduced, with the lowest THR value (22 kJ/g) obtained for PA6/5 % MgO/5 %EG and PA6/5 %RP/5 %EG samples. The time to pHRR also increased due to the effect of the flame retardants, with a delay of up to 167 s to the maximum heat release. In addition, the mass remaining after pyrolysis also increased compared to the reference, mainly due to the expandable graphite acting in the solid phase. It is observed that for the samples containing HPCTP and expandable graphite, the residual mass also increased with the amount of graphite. The heat release capacity (HRC) of the reference PA6 sample was 433 J/g·K. The HRC of the PA6/5 %MgO/5 %EG sample was almost unchanged, but the PA6/3P % HPCTP/3 %EG sample had 2 % higher HRC than the reference PA6. In contrast, the HRC of the PA6/5 %RP/5 %EG sample and the PA6/3P % HPCTP/4 %EG sample decreased by 12 % and 4 %, respectively.

3.2. Mass loss type cone calorimetry (MLC)

The flammability of reference and coated PA6 composites was tested using MLC. The results are summarised in Table 3, and the heat release of the samples versus time is shown in Fig. 5. The MLC results of coated composites have been partially presented in our previous publications [22,23], but in the present publication, the results have been complemented with MARHE and EHC results.

The reference PA6/CF sample ignited in 17 s, whereas the application of the flame retardant coatings extended the TTI. Particularly efficient was the PA6/CF/3P %HPCTP/4 %EG sample, where the TTI more than doubled compared to the reference (36 s). The pHRR of the PA6/CF sample was 347 kW/m^2, which was reduced by up to 33 % with 3 P % HPCTP and 3 % EG. The time to pHRR was reduced compared to the reference (164 s), except for the PA6/CF/3P %HPCTP/3 %EG sample. Observing the heat release curves in Fig. 5, the characteristics of the PA6/CF sample showed a sudden increase in heat release followed by a double peak. In contrast, the heat release of the samples with flame retardant coating had a smaller initial slope, and after the peak, the heat release started to decrease. This decrease indicates that the samples have rapidly formed a protective layer that prevents further heat release. For the PA6/CF/3P %HPCTP/4 %EG sample, no sharp peak was observed, but the heat release remained nearly constant after the initial increase, and then the curve started to decay after 200 s. The THR decreased with each of the flame retardant coatings. The lowest THR value was achieved for the PA6/CF/3P %HPCTP/4 %EG sample (57 MJ/m^2), which is 40 % lower than in the case of the reference sample (96 MJ/m^2). The residual mass increased significantly compared to the PA6/CF sample, which is due to the condensed phase mechanism of the expandable graphite. The PA6/CF/5 %RP/5 %EG sample had the highest residual mass, suggesting that the red phosphorus facilitated the charring process. The MARHE value decreased significantly with each of the flame retardant coatings. The coatings reduced the MARHE by 25–36 %, with the lowest value observed for the sample containing 3 P % HPCTP and 3 % EG. The EHC was also reduced by the coatings, with a maximum reduction of 52 % compared to the reference sample (67 MJ/kg) in the PA6/CF/3P %HPCTP/4 %EG formulation. For the PA6/CF/5 %MgO/5 %EG sample, the decrease in MARHE and EHC were almost identical (29 % and 32 %, respectively), suggesting that the main flame retardant mechanism is the condensed phase mechanism. In contrast, for the other samples (PA6/CF/5 %RP/5 %EG, PA6/CF/3P %HPCTP/3 %EG, PA6/CF/3P %HPCTP/4 %EG), the decrease in EHC is significantly larger than the decrease in MARHE, suggesting that the samples are characterised by a combined mechanism.

3.3. Scanning electron microscopy and energy dispersive X-ray spectroscopy (SEM-EDS)

The elemental composition of the residual samples after combustion by SEM-EDS provides insight into the solid-phase mechanism of action of the flame retardants and the synergistic effect between mixed-composition flame retardants. Similar trends were observed for all mixed compositions, therefore, only the results for the sample containing RP and EG are presented (Fig. 6).

The PA6 sample was almost completely burnt during the MLC test. The EDS image of the small amount of residual sample shows mainly

oxygen and also aluminium and sodium, which may have been remaining from the initiator. In addition to the mixed composition (PA6/CF/5 %RP/5 %EG), a sample with only 5 % EG and a sample with only 5 % RP were tested to allow a proper comparison and to investigate the combined effect of the flame retardants. In the case of the PA6/CF/5 %RP sample, a thin, continuous protective layer was formed after burning. Red phosphorus (RP) primarily acts in the condensed phase by promoting char formation, while it can also have a secondary effect in the gas phase through the release of phosphorus-containing radicals [24, 25]. In the EDS images (Fig. 6) that P and O are detected in the same positions, as phosphorus oxide is formed when RP is oxidised in the solid phase. This oxide can then react with water from the degradation of the material to form phosphoric acid or polyphosphoric acid, which coats the surface of the polymer [25]. The expansion of EG occurs through a redox reaction between H_2SO_4 intercalated between the graphite layers and the graphite itself. This reaction produces gases that cause a significant increase in volume when heated above 200 °C. The expansion of the graphite forms a structure similar to a "worm" (Fig. 6(c)), which effectively extinguishes the flame. In addition, the dense char layer limits the transfer of heat and mass from the material to the heat source, thus inhibiting further degradation of the polymer [26].

In the PA6/CF/5 %RP/5 %EG sample, a phosphorus-rich outer layer formed, while the inner part of the char, primarily composed of expandable graphite, also contained phosphorus. The presence of phosphorus contributed to a stable outer layer surrounding the expanded graphite, preventing the protective layer from breaking apart easily. According to the literature [27], by combining RP and expandable graphite after ignition, the expandable graphite forms a poor thermal conductivity layer, which protects PA6 from further thermal effects. In addition, as the temperature increases, the phosphorus starts to oxidise, and different P-containing groups are formed, which can further react with the graphite in the carbon layer under the influence of oxygen and heat, thus creating a more stable carbon layer.

The explanation for the different inner and outer layers is that the larger grains of expandable graphite have started to sediment on the bottom of the coating. As the heat expanded the expandable graphite, the heteroatoms were shifted to the outside of the coating. This process is shown schematically in Fig. 7.

Fig. 8 shows the P-content from RP (Fig. 8(a)), the Mg-content from MgO in atomic % (Fig. 8(b)) and the P-content from HPCTP (Fig. 8(c)) in the residues after burning. We investigated samples containing only one flame retardant (PA6/5 %RP, PA6/3P %HPCTP, PA6/5 %MgO) and the compositions in combination with expandable graphite. For the mixed compositions, the inner layer of the residue and the outer layer were also investigated separately. For the PA6/5 %RP sample and the PA6/5 %EG sample, there was no difference between the outer and inner part of the burn residue, so they were not analysed separately. For the PA6/5 %RP sample, the atomic % of P was 11, while for the PA6/5 %RP/5 %EG sample, the inner part contained 2 atomic %, and the outer part was 12 atomic % P. The P-content of the sample containing 3P % HPCTP was 15

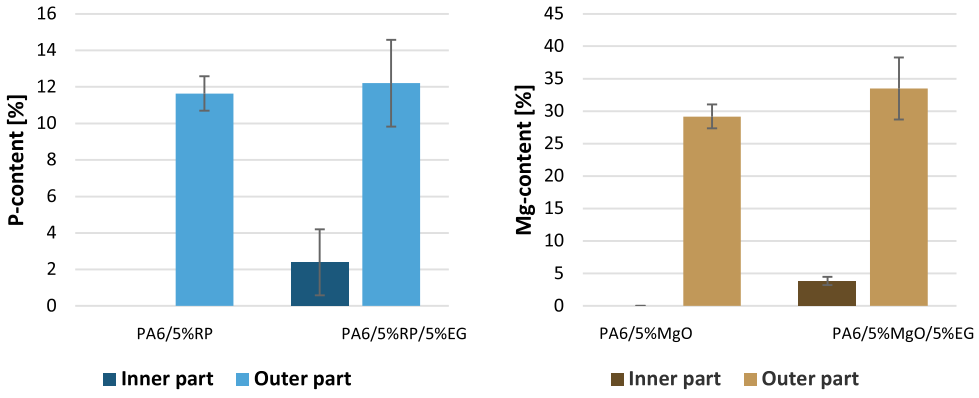

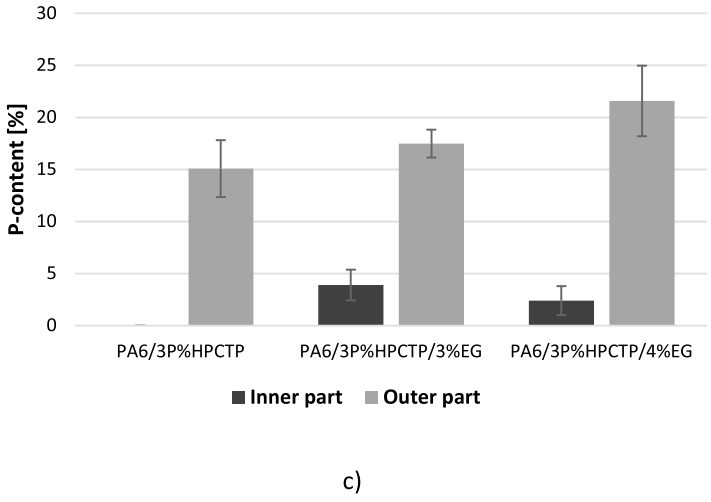

Fig. 8. Phosphorus and magnesium content in the post-combustion residue where a) sample PA6/5 %RP/5 %EG, b) sample PA6/5 %MgO/5 %EG, c) sample PA6/3P %HPCTP/3 %EG and PA6/3P %HPCTP/4 %EG.

atomic %, which increased to 18 atomic % with the addition of 3 % expandable graphite in the outer layer and to 22 atomic % with the addition of 4 % EG. The inner part of the PA6/3P %HPCTP/3 %EG sample contained 3.9 atomic % of P, while for the PA6/3P %HPCTP/4 % EG sample it was 2.4 atomic %. For Mg-content, a similar trend was observed, as compared to the PA6/5 %MgO sample (29.2 atomic%), the Mg-content increased to 33.5 atomic % in the outer part, while nearly 4 atomic % of Mg was detectable in the inner layer. The results show that with the addition of EG, all heteroatoms (P and Mg) are enriched in the outer layer, but they are also present in small amounts among the graphite flakes in the inner layer.

3.4. Laser pyrolysis - Fourier-transformed infrared spectrometry

The gases generated during pyrolysis of the reference sample and the coatings were identified by LP-FTIR. According to the literature [28], the degradation of PA6 mainly produces cyclic oligomers and monomers. The combustion process typically produces hydrogen cyanide (HCN), NOx, CO_2, CO and H_2O, of which HCN and CO are the main hazardous compounds. The gas-phase spectra of the reference and flame retardant compositions are shown in Fig. 9.

Pyrolysis products of PA6 had a peak at 3300 cm^{-1} corresponding to N-H stretching vibrations of amide groups. A high-intensity peak was observed around 1660 cm^{-1}, which is related to the C=O stretching of the amide I band. N-H bending and C-N stretching vibrations of the amide II band were identified around 1550 cm^{-1}. In addition, intense C-H stretching vibrations were observed in the 3200-2800 cm^{-1} range, indicating the presence of hydrocarbons. The decomposition of PA6 can produce hydrogen cyanide (HCN) with characteristic peaks around 3260 cm^{-1} and 2250 cm^{-1}. The peak at around 3260 cm^{-1} overlaps with the N-H stretching associated with amide groups, making it difficult to separate the two peaks, but at 2250 cm^{-1} a lower intensity peak appears, indicating the presence of HCN. A strong CO_2 absorption band in the 2400-2300 cm^{-1} range indicated an oxidation process and significant CO_2 emissions, while small amounts of carbon monoxide (CO) were also detected in the 2200-2080 cm-^{1} range. The results suggest that the pyrolysis of PA6 produces a substantial amount of combustible and toxic gases. A significant difference in the spectra of the PA6/5 %MgO/5 %EG sample compared to the reference is observed: The C-H stretching vibrations are almost absent, which may indicate that during oxidation, most of the combustible components are further oxidised to CO_2. This statement is supported by the formation of an intense CO_2 peak in the 2400-2300 cm^{-1} range, indicating large amounts of CO_2 emission, which suggests that the presence of MgO catalyses oxidation, leading to faster decomposition. The intensity of the amide I and amide II bands also decreased, suggesting that carbon retention in the solid phase increased, reducing the formation of volatile hydrocarbons and leading to char formation. In addition, EG can bind HCN, which may contribute to reducing toxic gas emissions. The intensity of C-H stretching vibrations (3200-2800 cm^{-1}) decreased in the PA6/5 %RP/5 %EG sample compared to the reference PA6 but to a lesser extent than in the PA6/5 % MgO/5 %EG sample. The intensity of the peaks associated with toxic HCN slightly decreased, and CO_2 emissions were lower than in the reference sample. A small shoulder appeared around 1178 cm^{-1}, which may be indicative of P-containing vibrations. This suggests that RP also exerts its effect to a small extent in the gas phase. According to the literature, RP in contact with oxygen forms PO· radicals, which can act as OH· and H· free radical scavengers in the gas phase, thus inhibiting flame propagation. In addition, the condensed phase effect of RP is also significant, as the polyphosphates form a thermally protective char layer that inhibits further heat transfer and reduces the formation of combustible gases. The peak in the spectrum of PA6/3P %HPCTP/3 % EG between 740-785 cm^{-1} is indicative of P-C vibrations, and the peak around 1178 cm^{-1} is indicative of P-O-C vibrations. The P=O vibrations would appear at 1264 cm^{-1}, which, however overlap with a peak at PA6. However, the presence of P=O oscillations may be indicated by the wider peak formed than the peak at PA6. A low-intensity peak around 960 and 930 cm^{-1} was observed, which may indicate ammonia (NH_3). Based on the literature [17], HPCTP decomposes into phosphorus and nitrogen free radicals, which act as reactive radical scavengers in the gas phase, binding the OH· and H· free radicals necessary to sustain the flame, thereby reducing the flame temperature and fire spread. As the amount of expandable graphite (EG) increased, the intensity of the C-H peaks (3100-2800 cm^{-1}) characteristic of aliphatic hydrocarbons decreased further, indicating that fewer combustible components were released. The CO_2 peak became lower than in the PA6/3P %HPCTP/3 %

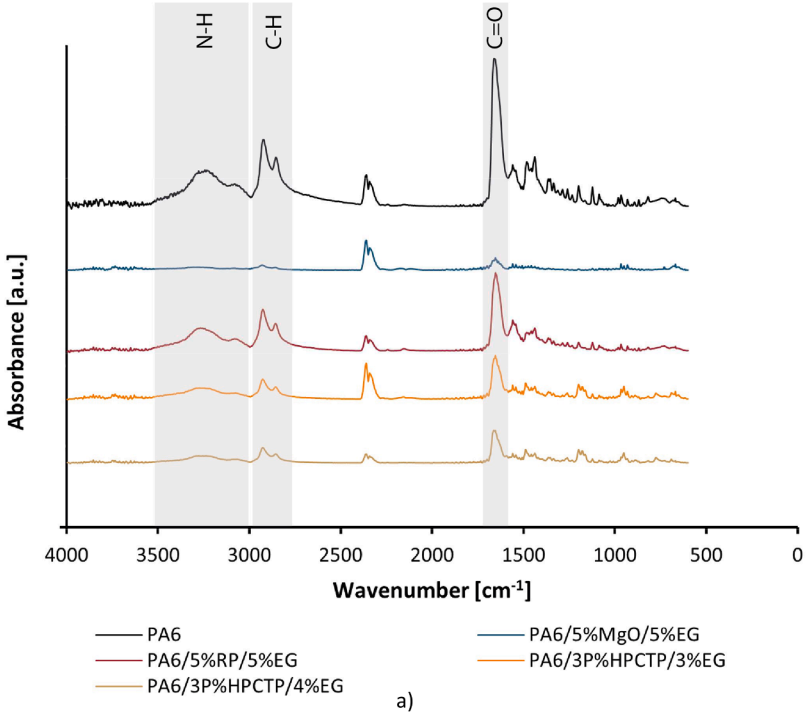

Fig. 9. Effects of flame retardants in the gas phase in LP-FTIR in the range of a) 4000-0 cm^{-1}, b) 1400-600 cm^{-1} and c) 2400-2000 cm^{-1}.

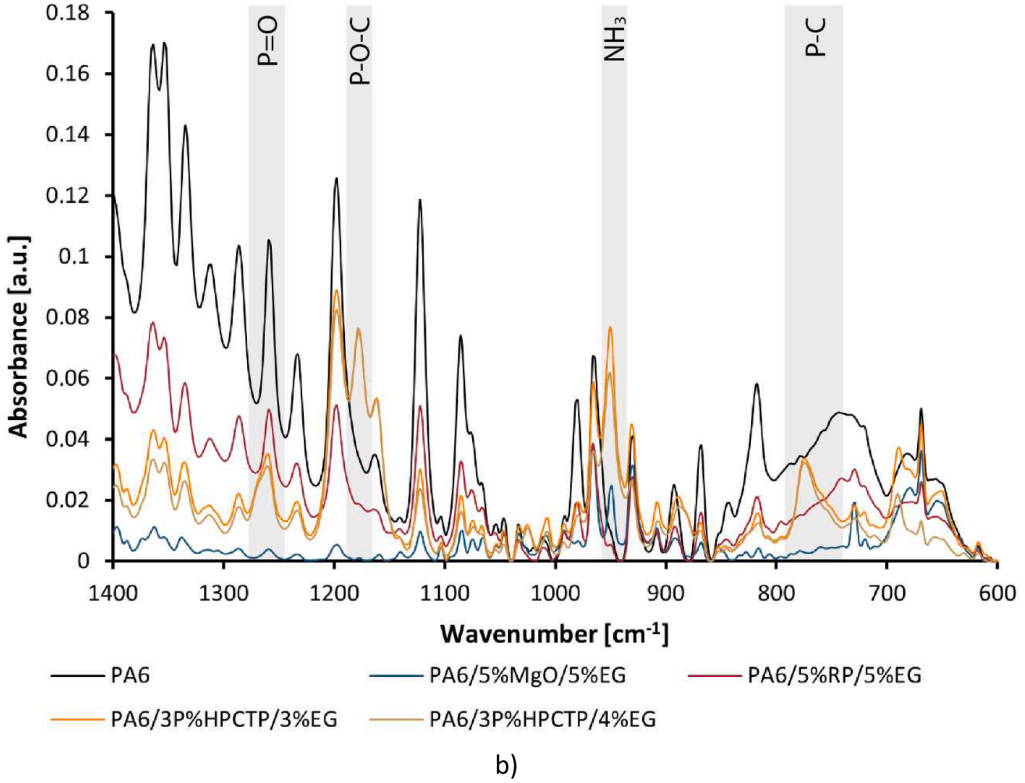

b)

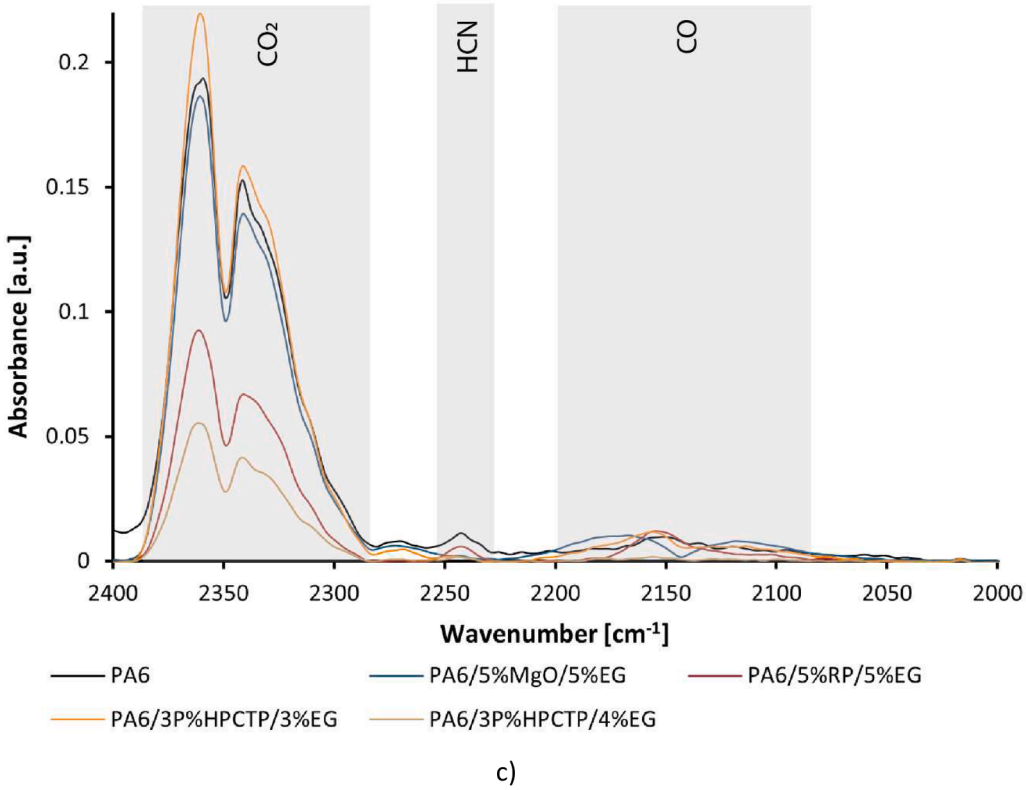

c)

Fig. 9. (*continued*).

EG sample, suggesting that less CO_2 was generated from oxidation and forming a solid protective layer dominated. In addition, the reduction of toxic HCN emissions was more effective. As in the PA6/3P %HPCTP/3 % EG sample, peaks associated with P-C and P-O-C vibrations appeared, as well as a broadened peak at 1264 cm^{-1} indicative of P=O vibrations.

3.5. Glow wire flammability index (GWFI)

The GWFI test was conducted on reference and coated carbon fibre-reinforced polyamide 6 (CF/PA6). This test is widely used in the electronics, electrical, and energy industries, particularly for evaluating the

Table 4
The results of GWFI measurements for reference and coated PA6 composites.

Sample	GWFI
PA6/CF	960/2
PA6/CF/5 %MgO/5 %EG	960/2.5
PA6/CF/5 %RP/5 %EG	960/2.5
PA6/CF/3P %HPCTP/3 %EG	960/2.5
PA6/CF/3P %HPCTP/4 %EG	960/2.5

fire resistance of plastic components in electrical enclosures, connectors, circuit breakers, and insulating materials. While it is primarily associated with these industries, it is also relevant in automotive applications, where PA6 composites are commonly used. With the rise of electric vehicles, flame resistance has become a significant concern. Therefore, the GWFI test plays a crucial role in certifying PA6 composites. The results of the test are summarised in Table 4. The first number in the GWFI value indicates the temperature, while the part after the '/' indicates the sample thickness.

Reference and flame retardant coated samples were tested at 500 °C, 550 °C, 600 °C, 650 °C, 700 °C, 750 °C, 800 °C, 850 °C, 900 °C and 960 °C. All samples passed the specifications of the standard at 960 °C, i.e., after 30 s of ignition, the flame was extinguished within 30 s, and the cotton tissue under the sample was not ignited. The reference PA6/CF composite ignited at 960 °C when the glow wire touched the sample. A 2-4 cm high flame was formed during combustion and continued to burn for 4 s after 30 s of ignition. The glow wire entered the test specimen by 1.5 mm. The PA6/CF/5 %MgO/5 %EG specimen ignited immediately after contact with the hot wire at 960 °C and continued to burn for 6 s with a 5-6 cm flame after 30 s of ignition. The PA6/CF/5 %RP/5 %EG sample also ignited following contact but continued to burn for only 2 s after ignition with a 4-5 cm flame. The PA6/CF/3P %HPCTP/3 %EG and PA6/CF/3P %HPCTP/4 %EG samples ignited immediately upon exposure to the 960 °C glow wire but were extinguished after 7 s and 5 s, respectively. Both samples were burned with a flame of 4-5 cm. For all the samples with flame retardant coatings, it was observed that the penetration depth was only 0.5 mm, i.e. the composite was not damaged by the glow wire, only the coating. It can also be said that all the samples did not ignite up to 750 °C but only smoked, while at 800 °C, they were extinguished immediately after the contact was broken. However, increasing the temperature did not result in a significant burn length.

3.6. Shore D hardness

The hardness of the flame retardant coatings was tested on the 6 mm thick coatings without the composite base. The explanation for this is that the 0.5 mm coating is not thick enough to test the hardness of the

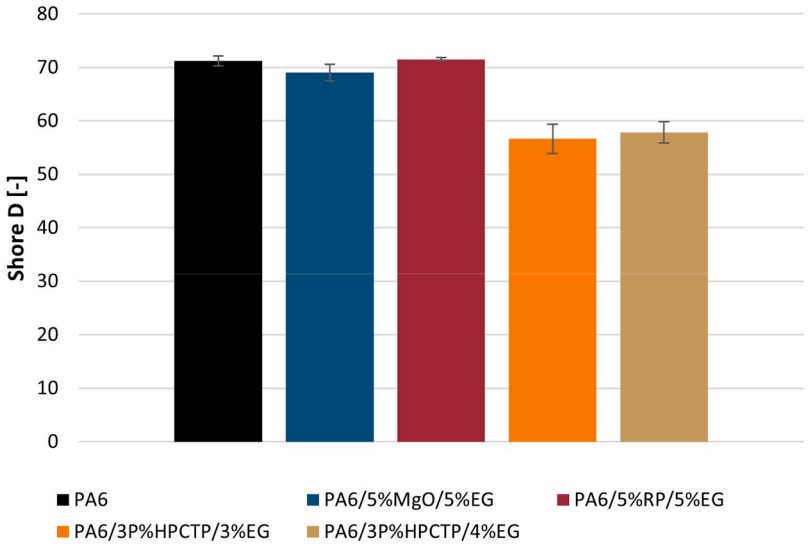

Fig. 10. Shore D hardness of reference and flame retardant coatings.

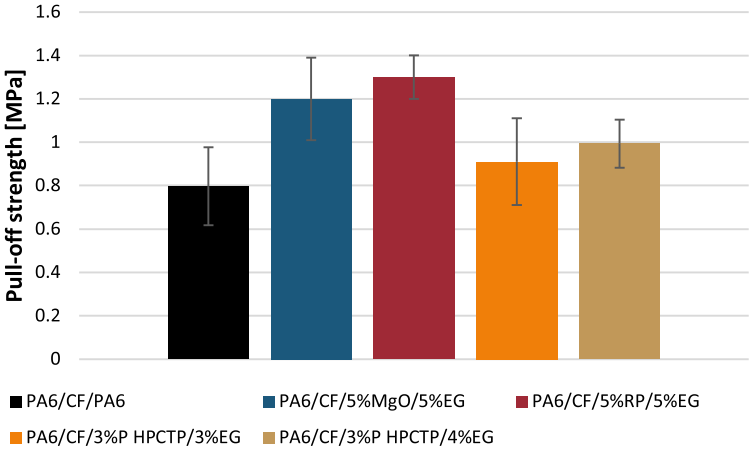

Fig. 11. Pull-off strength of reference and flame retardant coatings.

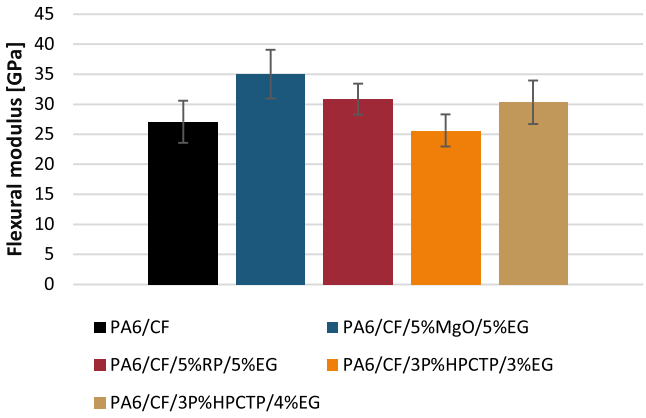

Fig. 12. Flexural modulus of reference and flame retardant coatings.

coating alone, so the hardness of the composite would affect the results. PA6 without flame retardant and reinforcement was used as a reference. The results obtained are presented in Fig. 10.

For the reference PA6 without flame retardant, a hardness of 71 Shore D was achieved, similar to the hardness values found in the literature [10]. Samples containing solid particulate flame retardants (PA6/5 %MgO/5 %EG, PA6/5 %RP/5 %EG) did not significantly affect the hardness, with 69 Shore D hardness for the sample containing MgO and 72 Shore D hardness for the sample containing RP. A significant difference was observed for coatings containing HPCTP, where the plasticising effect of HPCTP was evident. According to the literature [16], HPCTP acts as a plasticiser and weakens intermolecular interactions between polymer chains, such as hydrogen bonds. The average hardness of the coating containing 3P % HPCTP and 3 % EG was 57, and that of the coating containing 3 % HPCTP and 4 % EG was 58.

3.7. Pull-off test

When applying flame retardant coatings, proper adhesion between the composite and the coating is crucial. The pull-off strength of each coating is shown in Fig. 11. As a reference, a flame retardant-free PA6 coating was applied to a carbon fibre-reinforced PA6 composite using the same coating preparation method described in section 2.3.

Based on the pull-off test, it can be concluded that the coatings have approximately the same pull-off strength. Compared to the reference coating without flame retardants, the flame retardants slightly increased the pull-off strength, i.e., the adhesion between the composite and the coating improved. For samples containing HPCTP and EG, increasing the amount of EG increased the average pull-off strength by 0.1 MPa. From these results, it can be concluded that the solid particulate flame retardant does not significantly affect the adhesion between the coating and the composite. The PA6/CF/5 %RP/5 %EG sample had the highest adhesive strength (1.3 MPa).

If the failure occurs within the composite, it is called cohesive failure, and if it takes place at the interface between the composite and the coating, it is called adhesive failure. Adhesive failure was observed for all coated composites.

3.8. Three-point bending test

Three-point bending tests were conducted on PA6 composites with flame retardant coating, with an uncoated PA6 composite as a reference. In each case, the coated side was the compressive side for the samples with flame retardant coating. Flexural strength and flexural modulus are shown in Figs. 12 and 13, respectively.

The specimens did not break at a deflection of 10 % of the support spacing, so the limit bending stress was measured. The flame retardant coatings did not fracture after bending but separated from the composite surface at the compressed area. The limit bending stress of the samples containing RP and MgO did not change significantly compared to the reference. However, the effect of HPCTP decreased the interfacial tension. Similar to the Shore D hardness, the softening effect of HPCTP is also seen here. For samples containing 3P % HPCTP and 3 % EG, the interfacial tension is 151 MPa. The strength can also be increased by increasing the amount of expandable graphite (192 MPa). The highest ultimate yield stress was found for the PA6/5 %MgO/5 %EG sample, and its value was 255 MPa. The highest flexural modulus was also found for the PA6/5 %MgO/5 %EG sample (35 GPa).

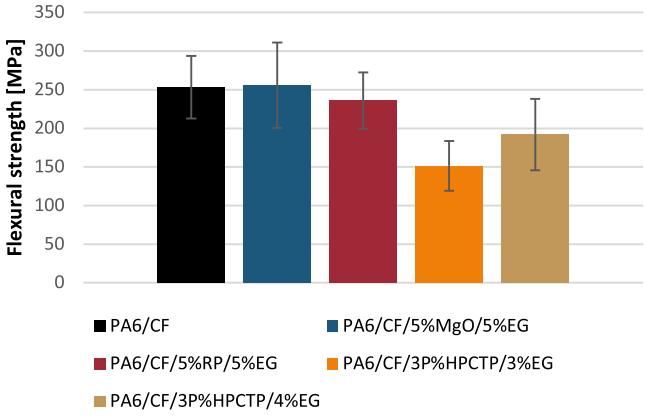

Fig. 13. Flexural strength of reference and flame retardant coatings.

Table 5
Mechanism of flame retardant in combined flame retardant coatings.

Sample	Gas phase (LP-FTIR)	Condensed phase (MLC residue, SEM-EDS)	MARHE [kW/m^{2}s] EHC [MJ/kg]	FR mechanism
PA6/CF/5 % MgO/ 5 %EG	Significantly reduced C-H elongations. Intense CO_2 peak and CO emissions. Reduced HCN peak. Mainly oxidation process.	Residue: 25 % increase Mg-content in the outer layer after the addition of EG: 15 % increase	MARHE: 29 % decrease EHC: 32 % decrease	Condensed phase mechanism: increased oxidation processes, reduced amount of flammable components
PA6/CF/5 % RP/5 %EG	Reduced C-H elongations. Minor CO_2 reduction and HCN reduction. P-containing compounds.	Residue: 36 % increase P-content in the outer layer after the addition of EG: 5 % increase	MARHE: 25 % decrease EHC: 46 % decrease	Combined mechanism: RP promotes the formation of a protective layer in the solid phase; P-containing radical scavengers in the gas phase
PA6/CF/3P % HPCTP/3 % EG	Reduced C-H elongations. P-containing compounds. NH_3 emissions	Residue: 28 % increase P-content in the outer layer after the addition of EG: 16 % increase	MARHE: 36 % decrease EHC: 52 % decrease	Combined mechanism: formation of a protective layer in the solid phase; radical scavenging compounds in the gas phase
PA6/CF/3P % HPCTP/4 % EG	Further decrease in C-H elongations. Decrease in CO_2 and HCN emissions. P-containing compounds	Residue: 28 % increase P-content in the outer layer after the addition of EG: 43 % increase	MARHE: 35 % decrease EHC: 52 % decrease	Combined mechanism: formation of a protective layer in the solid phase; radical scavenging compounds in the gas phase

4. Conclusions

In our research, carbon fibre reinforced polyamide 6 composites were prepared by anionic ring-opening polymerisation of caprolactam. A flame retardant coating was prepared on the surface of the composite using an in-mould coating. As flame retardants, expandable graphite was used with magnesium oxide or red phosphorus or hexaphenoxycyclotriphosphazene. The different flame retardant formulations were selected based on our previous research [22,23]. The flame retardant coatings significantly reduced the pHRR, THR, MARHE and EHC compared to the reference and increased the residual mass and ignition time. In the MLC test with sample PA6/CF/3P %HPCTP/3 %EG, up to 33 % reduction in pHRR and with sample PA6/CF/3P %HPCTP/4 %EG, 40 % reduction in THR can be achieved. From the residues remaining after burning, it was found that a stable outer protective layer was formed on the surface of the samples, consisting mainly of heteroatoms (P, Mg) and an inner layer containing mainly expandable graphite. The addition of expandable graphite leads to an enrichment of heteroatoms and an increase of up to 43 % in heteroatom content (P-content for PA6/3P % HPCTP/4 %EG samples) compared to samples without EG. From the study of the gas phase mechanism (LP-FTIR), we found that combining MgO and EG reduces the C-H vibrations and that MgO enhances the oxidation processes. In the PA6/5 %RP/5 %EG sample, low-intensity P-containing compounds appear, and C-H vibrations are reduced. For samples containing HPCTP, the peaks of P-containing compounds became more intense than for the RP-containing sample, and HCN emission was reduced while ammonia was also detected. Based on the flammability studies, it was found that a condensed phase mechanism characterised the PA6/5 %MgO/5 %EG sample, but the other samples showed a combined mechanism, as radical scavenging free radicals were formed along with the charred protective layer. A detailed description of the mechanism of the flame retardants in the combined coatings is summarised in Table 5, where the results are compared to the values of the coatings containing only a single additive (MgO, RP or HPCTP). In the GWFI test, all samples passed the requirements of the standard at 960 °C. When testing the Shore D hardness of the coatings, it was found that HPCTP has an annealing effect but that the hardness can be increased by increasing the amount of expandable graphite. The study of mechanical properties also revealed that HPCTP has a plasticising effect. Based on the findings of the experiments, it can be concluded that mixed composition flame retardant coatings can be effective in the flame retardancy of carbon-fibre reinforced PA6 composites, while the mechanical properties are not or only slightly modified and at the same time the negative effect of fibre reinforcement on the intumescent phenomena is eliminated.

CRediT authorship contribution statement

Zsófia Kovács: Writing – review & editing, Writing – original draft, Visualization, Validation, Methodology, Investigation, Conceptualization. **Andrea Toldy:** Writing – review & editing, Supervision, Resources, Project administration, Methodology, Funding acquisition, Conceptualization.

Declaration of competing interest

The authors declare that they have no known competing financial interests or personal relationships that could have appeared to influence the work reported in this paper.

Acknowledgements

This research was funded by the National Research, Development and Innovation Office (NKFIH K142517). Project no. TKP-6-6/PALY-2021 has been implemented with the support provided by the Ministry of Culture and Innovation of Hungary from the National Research, Development and Innovation Fund, financed under the TKP2021-NVA funding scheme.

Data availability

Data will be made available on request.

References

[1] M.-X. Li, H.-L. Mo, S.-K. Lee, Y. Ren, W. Zhang, S.-W. Choi, Rapid impregnating resins for fiber-reinforced composites used in the automobile industry, Polymers (Basel). 15 (2023) 4192, https://doi.org/10.3390/polym15204192.
[2] S. Mahboubizadeh, O. Ashkani, T. RezaTabrizi, M.H. Shekarabi, Importance and applications of fiber reinforced polymer composite in the transportation industry: A general review, Mater. Chem. Mech. 1 (2023) 16–26, https://doi.org/10.22034/mcm.2023.3.3.
[3] P. Csvila, T. Czigány, Multifunctional energy storage polymer composites: the role of nanoparticles in the performance of structural supercapacitors, Express Polym. Lett. 18 (2024) 1023–1038, https://doi.org/10.3144/expresspolymlett.2024.78.
[4] M. Baskaran, A. de la Calle, I. Harismendy, S. García-Arrieta, C. Elizetxea, L. Aretxabaleta, J. Aurrekoetxea, Impact performance comparison of carbon fiber reinforced polyamide 6 and fast-curing epoxy composites manufactured by resin transfer molding, Polym. Compos. (2024) 1–9, https://doi.org/10.1002/pc.29317.
[5] H. N, N. L, A.A. H, K. C, M. S, S. P, A review of long fibre thermoplastic (LFT) composites, Int. Mater. Rev. 65 (2020) 164–188, https://doi.org/10.1080/09506608.2019.1585004.
[6] C. Podara, S. Termine, M. Modestou, D. Semitekolos, C. Tsirogiannis, M. Karamitrou, A.-F. Trompeta, T.K. Milickovic, C. Charitidis, Recent trends of recycling and upcycling of polymers and composites: A comprehensive review, Recycling. 9 (2024) 37, https://doi.org/10.3390/recycling9030037.

[7] A. Toldy, Challenges and opportunities of polymer recycling in the changing landscape of European legislation, Express Polym. Lett. 17 (2023) 1081, https://doi.org/10.3144/expresspolymlett.2023.81.
[8] A. Kausar, Advances in carbon fiber reinforced polyamide-based composite materials, Adv. Mater. Sci. 19 (2019) 67–82, https://doi.org/10.2478/adms-2019-0023.
[9] Z. Gao, R. Zhao, S. Cai, X. Ning, An applicability study on various methods for determiningthe monomer conversion rate of polyamide 6, J. Appl. Polym. Sci. 141 (2023) e55487, https://doi.org/10.1002/app.55487.
[10] O.V. Semperger, A. Suplicz, The effect of the parameters of T-RTM on the properties of polyamide 6 prepared by in situ polymerization, Mater. (Basel) 13 (2019) 4, https://doi.org/10.3390/ma13010004.
[11] J. Lagarinhos, S.M. da Silva, J.M. Oliveira, Non-isothermal crystallization kinetics of polyamide 6/graphene nanoplatelets nanocomposites obtained via in situ polymerization: effect of nanofiller size, Polymers (Basel) 15 (2023) 4109.
[12] G. Fredi, L. Broggio, M. Valentini, M. Bortolotti, D. Rigotti, A. Dorigato, A. Pegoretti, Decoding the interplay of mold temperature and catalysts concentration on the crystallinity and mechanical properties of anionic polyamide 6: a combined experimental and statistical approach, Polymer (Guildf) 331 (2024) 127562, https://doi.org/10.1016/j.polymer.2024.127562.
[13] J. Gao, Y. Wu, J. Li, X. Peng, D. Yin, H. Jin, S. Wang, J. Wang, X. Wang, M. Jin, Z. Yao, A review of the recent developments in flame-retardant nylon composites, Compos. Part C Open Access. 9 (2022) 100297, https://doi.org/10.1016/j.jcomc.2022.100297.
[14] Z. Kovács, Á. Pomázi, A. Toldy, The flame retardancy of polyamide 6—Prepared by in situ polymerisation of ε-caprolactam—For T-RTM applications, Polym. Degrad. Stab. 195 (2022) 109797, https://doi.org/10.1016/j.polymdegradstab.2021.109797.
[15] J. Doležal, V. Benešová, J. Brožek, Preparation of polyamide 6 with reduced flammability by polymerization casting, J. Therm. Anal. Calorim. 149 (2023) 981–991, https://doi.org/10.1007/s10973-023-12774-1.
[16] C.-C. Höhne, R. Wendel, B. Käbisch, T. Anders, Hexaphenoxycyclotriphosphazene as FR for CFR anionic PA6 via T-RTM a study of mechanical and thermal properties, Fire Mater. 41 (2016) 291–306, https://doi.org/10.1002/fam.2375.
[17] C. Yan, P. Yan, H. Xu, D. Liu, G. Chen, G. Cai, Y. Zhu, Preparation of continuous glass fiber/polyamide6 composites containing hexaphenoxycyclotriphosphazene: mechanical properties, thermal stability, and flameretardancy, Polym. Compos. 43 (2021) 1022–1037, https://doi.org/10.1002/pc.26431.
[18] A. Toldy, B. Szolnoki, G. Marosi, Flame retardancy of fibre-reinforced epoxy resin composites for aerospace applications, Polym. Degrad. Stab. 96 (2011) 371–376, https://doi.org/10.1016/j.polymdegradstab.2010.03.021.
[19] A. Toldy, Flame retardancy of carbon fibre reinforced composites, EXPRESS Polym. Lett. 12 (2018) 186, https://doi.org/10.3144/expresspolymlett.2018.17.
[20] Á. Pomázi, A. Toldy, Multifunctional gelcoats for fiber reinforced composites, Coatings 9 (2019) 173, https://doi.org/10.3390/coatings9030173.
[21] O.V. Semperger, D. Török, A. Suplicz, Development and analysis of an in-mold coating procedure for thermoplastic resin transfer molding to produce PA6 composites with a multifunctional surface, Period. Polytech. Mech. Eng. 66 (2022) 350–360, https://doi.org/10.3311/PPme.21048.
[22] Z. Kovács, A. Toldy, Development of flame retardant coatings containing hexaphenoxycyclotriphosphazene and expandable graphite for carbon fibre-reinforced polyamide 6 composites, Polym. Degrad. Stab. 230 (2024) 111017, https://doi.org/10.1016/j.polymdegradstab.2024.111017.
[23] Z. Kovács, A. Toldy, Synergistic flame retardant coatings for carbon fibre-reinforced polyamide 6 composites based on expandable graphite, red phosphorus, and magnesium oxide, Polym. Degrad. Stab. 222 (2024) 110696, https://doi.org/10.1016/j.polymdegradstab.2024.110696.
[24] Q. Wu, J. Lü, B. Qu, Preparation and characterization of microcapsulated red phosphorus and its flame-retardant mechanism in halogen-free flame retardant polyolefins, Polym. Int. 52 (2003) 1326–1331, https://doi.org/10.1002/pi.1115.
[25] D. Zhou, W. He, N. Wang, X. Chen, J. Guo, S. Ci, Effect of thermo-oxidative aging on the mechanical and flame retardant properties of long glass fiber-reinforced polypropylene composites filled with red phosphorus, Polym. Compos. 39 (2016) 2634–2642, https://doi.org/10.1002/pc.24253.
[26] W.W. Focke, H. Badenhorst, W. Mhike, H.J. Kruger, D. Lombaard, Characterization of commercial expandable graphite fire retardants, Thermochim. Acta. 584 (2014) 8–16, https://doi.org/10.1016/j.tca.2014.03.021.
[27] N. Wang, L. Li, Y. Xu, K. Zhang, X. Chen, H. Wu, Synergistic effects of red phosphorus masterbatch with expandable graphite on the flammability and thermal stability of polypropylene/thermoplastic polyurethane blends, Polym. Polym. Compos. 28 (2019) 209–219, https://doi.org/10.1177/0967391119869552.
[28] H. Feuchter, F. Poutch, A. Beard, The impact of halogen free phosphorus, inorganic and nitrogen flame retardants on the toxicity and density of smoke from 10 common polymers, Fire Mater. 47 (2023) 1003–1023, https://doi.org/10.1002/fam.3145.